

CONSTRAINING ANISOTROPIC LORENTZ VIOLATION VIA THE SPECTRAL-LAG TRANSITION OF GRB 160625B

JUN-JIE WEI,^{1,2} XUE-FENG WU,^{1,3,4} BIN-BIN ZHANG,^{5,6} LANG SHAO,^{7,1} PETER MÉSZÁROS,^{8,9,10} AND V. ALAN KOSTELECKÝ¹¹

¹Purple Mountain Observatory, Chinese Academy of Sciences, Nanjing 210008, China; xfwu@pmo.ac.cn

²Guangxi Key Laboratory for Relativistic Astrophysics, Nanning 530004, China

³School of Astronomy and Space Science, University of Science and Technology of China, Hefei, Anhui 230026, China

⁴Joint Center for Particle, Nuclear Physics and Cosmology, Nanjing University-Purple Mountain Observatory, Nanjing 210008, China

⁵Instituto de Astrofísica de Andalucía (IAA-CSIC), P.O. Box 03004, E-18080 Granada, Spain

⁶Scientist Support LLC, Madsion, AL 35758, USA

⁷Department of Space Sciences and Astronomy, Hebei Normal University, Shijiazhuang 050024, China

⁸Department of Astronomy and Astrophysics, Pennsylvania State University, 525 Davey Laboratory, University Park, PA 16802, USA

⁹Department of Physics, Pennsylvania State University, 104 Davey Laboratory, University Park, PA 16802, USA

¹⁰Center for Particle and Gravitational Astrophysics, Institute for Gravitation and the Cosmos, Pennsylvania State University, 525 Davey Laboratory, University Park, PA 16802, USA

¹¹Physics Department, Indiana University, Bloomington, IN 47405, USA; kostelec@indiana.edu

Draft version May 30, 2017

ABSTRACT

Violations of Lorentz invariance can lead to an energy-dependent vacuum dispersion of light, which results in arrival-time differences of photons arising with different energies from a given transient source. In this work, direction-dependent dispersion constraints are obtained on nonbirefringent Lorentz-violating effects, using the observed spectral lags of the gamma-ray burst GRB 160625B. This burst has unusually large high-energy photon statistics, so we can obtain constraints from the true spectral time lags of bunches of high-energy photons rather than from the rough time lag of a single highest-energy photon. Also, GRB 160625B is the only burst to date having a well-defined transition from positive lags to negative lags, which provides a unique opportunity to distinguish Lorentz-violating effects from any source-intrinsic time lag in the emission of photons of different energy bands. Our results place comparatively robust two-sided constraints on a variety of isotropic and anisotropic coefficients for Lorentz violation, including first bounds on Lorentz-violating effects from operators of mass dimension ten in the photon sector.

Subject headings: astroparticle physics — gamma-ray burst: individual (GRB 160625B) — gravitation — relativity

1. INTRODUCTION

Lorentz invariance is the foundational symmetry of Einstein's relativity. However, deviations from Lorentz symmetry at the Planck energy scale $E_{\text{Pl}} = \sqrt{\hbar c^5/G} \simeq 1.22 \times 10^{19}$ GeV are predicted in various quantum gravity theories attempting to unify General Relativity and quantum mechanics (Kostelecký & Samuel 1989; Kostelecký & Potting 1991, 1995; Mattingly 2005; Bluhm 2006; Amelino-Camelia 2013; Tasson 2014). The prospect of discovering Lorentz violation in nature via sensitive relativity tests has motivated numerous recent experimental searches. A compilation of results can be found in Kostelecký & Russell (2017).

Although any deviations from Lorentz symmetry are expected to be tiny at attainable energies $\ll E_{\text{Pl}}$, they can become detectable when particles travel over large distances. Astrophysical observations involving long baselines can therefore provide exceptionally sensitive tests of Lorentz invariance. In the photon sector, signatures of Lorentz violation include vacuum dispersion and vacuum birefringence, along with direction-dependent effects (Kostelecký & Mewes 2008). Vacuum dispersion produces a frequency-dependent velocity of the photon. Lorentz invariance can therefore be tested by comparing the arrival time differences of photons at different wavelengths originating from the same astrophysical source (see, e.g., Amelino-Camelia et al. 1998; Pavlopoulos 2005; Ellis et al. 2006; Jacob & Piran 2008; Kostelecký & Mewes 2008, 2009; Abdo et al. 2009; Vasileiou et al. 2013; Ellis & Mavromatos

2013; Kislat & Krawczynski 2015; Wei et al. 2017). Similarly, vacuum birefringence results in an energy-dependent rotation of the polarization plane of linearly polarized photons. Thus, astrophysical polarization measurements can also be used to test Lorentz invariance (see, e.g., Kostelecký & Mewes 2001, 2006, 2007, 2013; Gubitosi et al. 2009; Stecker 2011; Laurent et al. 2011; Toma et al. 2012; Kislat & Krawczynski 2017). Since polarization measurements are more sensitive than vacuum dispersion time-of-flight measurements by a factor $\propto 1/E$, where E is the energy of the light, polarization measurements typically yield more stringent limits (Kostelecký & Mewes 2009). However, many predicted signals of Lorentz violation have no vacuum birefringence, so limits from time-of-flight measurements are essential in a broad-based search for effects.

At attainable energies, violations of Lorentz invariance are described by the Standard-Model Extension (SME), which is the comprehensive realistic effective field theory characterizing Lorentz and CPT violation (Colladay & Kostelecký 1997, 1998; Kostelecký 2004). Each term in the SME Lagrange density consists of a Lorentz-violating operator of definite mass dimension d in natural units ($\hbar = c = 1$), contracted with a coefficient that governs the size of any observable effects. For arbitrary d , all terms affecting photon propagation have been constructed explicitly (Kostelecký & Mewes 2009). Photon vacuum dispersion is induced by operators of dimension $d \neq 4$ and is proportional to $(E/E_{\text{Pl}})^{d-4}$. Lorentz-violating terms with odd d violate CPT symmetry, while those with even d preserve CPT. For odd d , vacuum dispersion and

birefringence always occur together, whereas for each even d there is a subset of $(d-1)^2$ nonbirefringent but dispersive Lorentz-violating operators. The latter form an ideal target for time-of-flight measurements. In this paper, we focus on measuring coefficients controlling nonbirefringent dispersion with even $d = 6, 8, \text{ and } 10$.

In a previous paper (Wei et al. 2017), we derived new limits on isotropic linear and quadratic leading-order Lorentz-violating vacuum dispersion using the gamma-ray burst GRB 160625B, which is the only one to date known to display a well-defined transition from positive spectral lags to negative spectral lags. Spectral lag is the arrival-time difference either of a given feature such as a peak in light curves from the same source in different energy bands or of high- and low-energy photons, and it is a common observational feature in gamma-ray bursts (see, e.g., Cheng et al. 1995; Norris et al. 1996; Band 1997). In our conventions, a positive spectral lag corresponds to an earlier arrival time for the higher-energy photons. The restriction to isotropic vacuum dispersion disregards $d(d-2)$ possible effects from anisotropic violations at each d in a nonbirefringent scenario. In this paper, we use the peculiar time-of-flight measurements of GRB 160625B to constrain combinations of nonbirefringent Lorentz-violating coefficients with mass dimension $d = 6, 8, \text{ and } 10$, allowing for all direction-dependent effects.

To date, limits on the 25 $d = 6$ nonbirefringent coefficients for Lorentz violation have been obtained by studying the dispersion of light in observations of GRB 021206 (Boggs et al. 2004; Kostelecký & Mewes 2008), GRB 080916C (Abdo et al. 2009; Kostelecký & Mewes 2009), GRB 090510 (Fermi LAT & GBM Collaborations 2010), four bright gamma-ray bursts (Vasileiou et al. 2013), the blazar Markarian 501 (MAGIC Collaboration 2008; Kostelecký & Mewes 2008), the active galaxy PKS 2155-304 (Aharonian et al. 2008; Kostelecký & Mewes 2009), and 25 active galaxy nuclei (Kislat & Krawczynski 2015). Only three bounds have been obtained on combinations of the 49 $d = 8$ coefficients for nonbirefringent vacuum dispersion, derived from GRB 021206 (Boggs et al. 2004; Kostelecký & Mewes 2008), GRB 080916C (Abdo et al. 2009; Kostelecký & Mewes 2009), and GRB 090510 (Fermi LAT & GBM Collaborations 2010). No constraints have been placed on the 81 $d = 10$ coefficients. A compilation of the current limits in the literature can be found in Kostelecký & Russell (2017). While these constraints have reached high precision, most are obtained by concentrating on the time delay induced by Lorentz violation and neglecting the intrinsic time delays that depend on the emission mechanism of the astrophysical sources. Furthermore, the limits from gamma-ray bursts are based on the rough time lag for a single GeV-scale photon. Performing a search for Lorentz violation using true time lags of high-quality and high-energy light curves in multi-photon bands of different energy is therefore both timely and crucial.

In this work, by fitting the true multi-photon spectral-lag data of GRB 160625B, we give both a plausible description of the intrinsic energy-dependent time lag and robust constraints on Lorentz-violating coefficients with $d = 6, 8, \text{ and } 10$. In Section 2, we present an overview of the theoretical foundation of vacuum dispersion due to Lorentz violation. The data analysis and our results constraining coefficients for Lorentz violation are presented in Section 3. A brief summary and discussion are provided in Section 4.

2. VACUUM DISPERSION IN THE STANDARD-MODEL EXTENSION

In the SME framework, the modified dispersion relations for photon propagation *in vacuo* take the form (Kostelecký & Mewes 2008, 2009)

$$E(p) \simeq \left(1 - \zeta^0 \pm \sqrt{(\zeta^1)^2 + (\zeta^2)^2 + (\zeta^3)^2}\right) p, \quad (1)$$

where p is the photon momentum. The quantities $\zeta^0, \zeta^1, \zeta^2,$ and ζ^3 are momentum- and direction-dependent combinations of coefficients for Lorentz violation that can be decomposed in a spherical basis to yield

$$\begin{aligned} \zeta^0 &= \sum_{djm} p^{d-4} {}_0Y_{jm}(\hat{\mathbf{n}}) c_{(I)jm}^{(d)}, \\ \zeta^1 \pm i\zeta^2 &= \sum_{djm} p^{d-4} {}_{\mp 2}Y_{jm}(\hat{\mathbf{n}}) \left(k_{(E)jm}^{(d)} \mp ik_{(B)jm}^{(d)} \right), \\ \zeta^3 &= \sum_{djm} p^{d-4} {}_0Y_{jm}(\hat{\mathbf{n}}) k_{(V)jm}^{(d)}, \end{aligned} \quad (2)$$

where $\hat{\mathbf{n}}$ points towards the source and ${}_sY_{jm}(\hat{\mathbf{n}})$ are spin-weighted harmonics of spin weight s . The standard spherical polar coordinates (θ, ϕ) associated with $\hat{\mathbf{n}}$ are defined in a Sun-centered celestial-equatorial frame (Kostelecký & Mewes 2002), with $\theta = (90^\circ - \text{Dec.})$ and $\phi = \text{R.A.}$, where the astrophysical source is at right ascension R.A. and declination Dec.

The above decomposition characterizes all types of Lorentz violations for vacuum propagation in terms of four sets of spherical coefficients. For even d , the coefficients are $c_{(I)jm}^{(d)}, k_{(E)jm}^{(d)}, k_{(B)jm}^{(d)}$ and control CPT-even effects. For odd d , the coefficients are $k_{(V)jm}^{(d)}$ and govern CPT-odd effects. For example, in the isotropic limit the group-velocity defect for photons is found to be

$$\delta v_g \simeq \frac{1}{\sqrt{4\pi}} \sum_d (d-3) E^{d-4} \left(-c_{(I)00}^{(d)} \pm k_{(V)00}^{(d)} \right), \quad (3)$$

where the factor $(d-3)$ reflects the difference between group and phase velocities and is included here because its significance grows with larger values of d . Birefringence results when the usual degeneracy among polarizations is broken, for which at least one of $k_{(E)jm}^{(d)}, k_{(B)jm}^{(d)},$ or $k_{(V)jm}^{(d)}$ is nonzero. The only coefficients for nonbirefringent vacuum dispersion are $c_{(I)jm}^{(d)}$, which are therefore the focus of the present work. Note that all the spherical coefficients can be taken to be constants in the Sun-centered frame.

For even $d > 4$, nonzero values of $c_{(I)jm}^{(d)}$ lead to an energy dependence of the photon velocity in vacuum, so two photons of different energies $E_h > E_l$ emitted simultaneously from an astrophysical source at redshift z would arrive at Earth at different times. Setting to zero the coefficients for birefringent propagation, the group-velocity defect is given by

$$\delta v_g = - \sum_{djm} (d-3) E^{d-4} {}_0Y_{jm}(\hat{\mathbf{n}}) c_{(I)jm}^{(d)}, \quad (4)$$

which includes direction-dependent effects. The induced

arrival-time difference can therefore be written as

$$\begin{aligned} \Delta t_{LV} &= t_l - t_h \\ &\approx -(d-3) (E_h^{d-4} - E_l^{d-4}) \int_0^z \frac{(1+z')^{d-4}}{H_{z'}} dz' \sum_{jm} {}_0Y_{jm}(\hat{\mathbf{n}}) c_{(l)jm}^{(d)}, \end{aligned} \quad (5)$$

where t_h and t_l are the arrival times of the high-energy photons and the low-energy photons, respectively. Also, $H_z = H_0 [\Omega_m(1+z)^3 + \Omega_\Lambda]^{1/2}$ is the Hubble expansion rate at z , where the standard flat Λ CDM model with parameters $H_0 = 67.3 \text{ km s}^{-1} \text{ Mpc}^{-1}$, $\Omega_m = 0.315$, and $\Omega_\Lambda = 1 - \Omega_m$ is adopted (Planck Collaboration 2014). Note that the coefficients $c_{(l)jm}^{(d)}$ can be either positive or negative, contributing to a decrease or an increase in photon velocity with increasing photon energy, respectively. For example, when $\sum_{jm} {}_0Y_{jm}(\hat{\mathbf{n}}) c_{(l)jm}^{(d)}$ is positive, photons with higher energies would arrive on Earth after those with lower ones, implying a negative spectral lag due to Lorentz violation.

3. CONSTRAINTS ON SME COEFFICIENTS

In this section, we use the observation of GRB 160625B to place direction-dependent bounds on combinations of the coefficients $c_{(l)jm}^{(6)}$, $c_{(l)jm}^{(8)}$, and $c_{(l)jm}^{(10)}$. GRB 160625B was detected by the *Fermi* satellite on 2016 June 25 at $T_0 = 22 : 40 : 16.28$ UT, with coordinates (J2000) R.A.=308° and Dec.=+6.9° (Burns 2016; Dirirsa et al. 2016). Its redshift is $z = 1.41$ (Xu et al. 2016). This gamma-ray burst is special because its gamma-ray light curve consists of three dramatically different isolated sub-bursts with very high photon statistics (Burns 2016; Zhang et al. 2016). Since the second sub-burst of GRB 160625B is extremely bright, its light curve in different energy bands can be readily extracted. With multi-photon energy bands, Wei et al. (2017) calculated the spectral time lags in the light curves recorded in the lowest-energy band (10–12 keV) relative to any of the other light curves in higher-energy bands, finding that the observed lag Δt_{obs} increases at $E \lesssim 8$ MeV and then gradually decreases in the energy range $8 \text{ MeV} \lesssim E \lesssim 20 \text{ MeV}$. Table 1 of Wei et al. (2017) contains the 37 energy-lag measurements obtained from this analysis. The lag behavior is shown in Fig. 1 and is very peculiar, being the first transition from positive to negative lags discovered within a burst. Note that the spectral-lag analysis is restricted to the data from the Gamma-Ray Monitor on board the *Fermi* satellite. In principle, stronger constraints on coefficients for Lorentz violation could be derived by including the higher-energy photons detected by the *Fermi* Large Area Telescope (LAT). However, the LAT data are much sparser in terms of photon number, and there are only ten > 1 GeV LAT photons during the second sub-burst of GRB 160625B (Zhang et al. 2016). This makes it challenging to extract the LAT-band light curve with high temporal resolution and requires additional assumptions in the error analysis beyond those adopted here. A future large set of higher-energy data could permit further improvements over the results we report below.

Since the time delay Δt_{LV} induced by Lorentz violation is likely to be accompanied by an intrinsic energy-dependent time delay Δt_{int} caused by unknown properties of the source (see, e.g., Ellis et al. 2006; Biesiada & Piórkowska 2009), the observed time lag between two different energy bands should include two parts,

$$\Delta t_{\text{obs}} = \Delta t_{\text{int}} + \Delta t_{LV}. \quad (6)$$

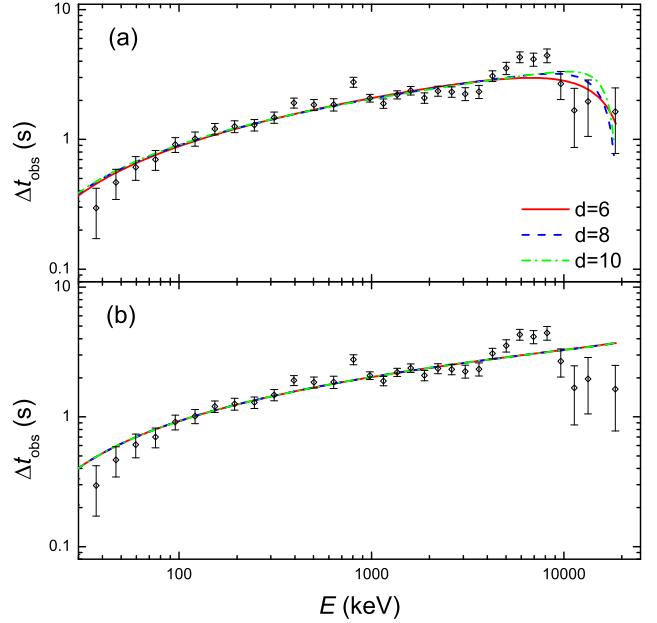


FIG. 1.— Panel (a): energy dependence of the observed spectral lag Δt_{obs} of the second sub-burst of GRB 160625B relative to the lowest-energy band, and the best-fit theoretical curves for the negative-lag case. Solid line: model with $d = 6$ coefficients. Dashed line: model with $d = 8$ coefficients. Dash-dotted line: model with $d = 10$ coefficients. Panel (b): same but for the positive-lag case.

As the spectral lags of most gamma-ray bursts have a positive energy dependence, with high-energy photons arriving earlier than the low-energy ones (see Minaev et al. 2014; Shao et al. 2016), we propose that the observer-frame relationship between the intrinsic time lag and the energy E is approximately a power law with positive dependence,¹

$$\Delta t_{\text{int}}(E) = \tau \left[\left(\frac{E}{\text{keV}} \right)^\alpha - \left(\frac{E_1}{\text{keV}} \right)^\alpha \right] \text{ s}, \quad (7)$$

where $\tau > 0$ and $\alpha > 0$, and where $E_1 = 11.34 \text{ keV}$ is the median value of the fixed lowest-energy band (10–12 keV). Also, Lorentz violation with positive $\sum_{jm} {}_0Y_{jm}(\hat{\mathbf{n}}) c_{(l)jm}^{(d)}$ implies high-energy photons arrive later than low-energy ones, so the positive correlation between the lag and the energy should gradually turn negative as the Lorentz violation becomes dominant at higher energies. The combined contributions from the intrinsic time lag and the Lorentz-violation lag can therefore lead to the observed lag behavior with a transition from positive to negative lags (Wei et al. 2017).

For the present analysis, we fit Eqs. (5), (6), and (7) to the 37 energy-lag measurements of GRB 160625B using the standard minimum χ^2 statistic. The parameters τ and α are allowed to be free and are fitted simultaneously with the combination $\sum_{jm} {}_0Y_{jm}(\hat{\mathbf{n}}) c_{(l)jm}^{(d)}$ of SME coefficients to yield best-fit values and uncertainties. Since the scenarios with positive and negative spectral lag due to Lorentz violation produce qualitatively different curves, we study the two cases separately. The

¹ Statistically, the intrinsic time lags of most GRBs increase with the energies E in the form of an approximate power-law function (e.g., Ellis et al. 2006; Biesiada & Piórkowska 2009), i.e., the power-law model is in fact an accurate representation of the energy dependence of the spectral lag.

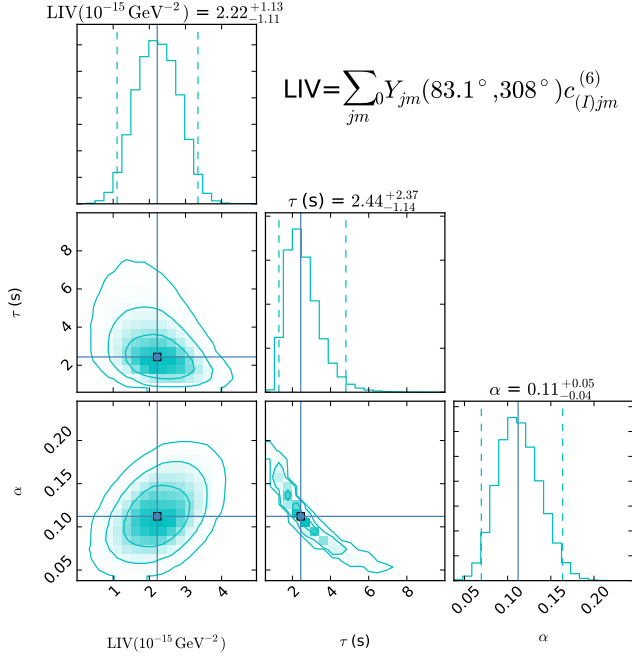


FIG. 2.— 1-D probability distributions and 2-D regions with the 1σ to 3σ contours corresponding to the parameters τ , α and vacuum coefficients with $d = 6$ for the negative-lag case. The vertical solid lines indicate the best-fit values. Made with triangle.py from Foreman-Mackey et al. (2013).

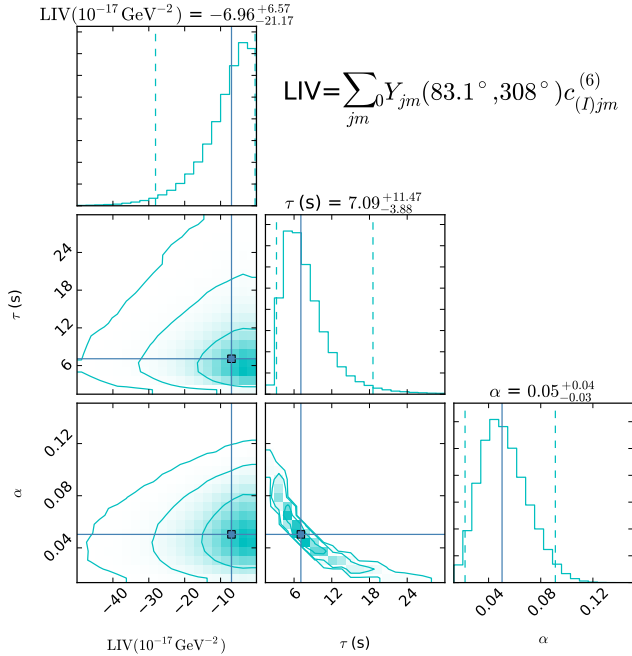


FIG. 3.— Same as Fig. 2, but for the positive-lag case.

data from GRB 160625B contain an apparent transition to a negative lag at high energies (see Fig. 1), so the strongest constraints can be expected in fitting for Lorentz violation with positive lag.

The results of the various fits are presented in Table 1. The cases of negative and positive Lorentz-violating spectral lag are displayed separately. For each value $d = 6, 8, 10$ in turn, the best-fit results and 2σ uncertainties are pro-

vided for the parameters τ and α and for the combination $\sum_{jm} Y_{jm}(\hat{\mathbf{n}}) c_{(l)jm}^{(d)}$ of coefficients for Lorentz violation, along with the χ^2 value for the fit. The latter values imply that nonzero Lorentz violation with $d = 6, 8, \text{ or } 10$ cannot be inferred from the data, so the results are most usefully expressed as constraints. The lower part of Table 1 gives two-sided estimated constraints at the 95% confidence level on each of the direction-dependent combinations of coefficients for Lorentz violation. We also provide estimated constraints at the 95% confidence level for the limiting case of isotropic Lorentz violation, where only the coefficients with $j = m = 0$ are relevant.

To illustrate the fits, the theoretical curves obtained from each of the best-fit values are provided in Fig. 1 for Lorentz violation contributing to both negative and positive lag. Also, the probability distributions for the analysis with $d = 6$ coefficients are shown in Fig. 2 for the scenario of negative lag due to Lorentz violation and in Fig. 3 for positive lag. These figures show the one-dimensional probability distribution for each free parameter and the two-dimensional contour plots with 1σ to 3σ confidence regions for the two-parameter combinations. The corresponding distributions for the $d = 8$ and 10 cases are qualitatively similar. As expected, the spreads of the distributions involving negative values of the combination $\sum_{jm} Y_{jm}(\hat{\mathbf{n}}) c_{(l)jm}^{(d)}$ are much larger than those for positive values, reflecting the occurrence at high energies of the negative lag transition in the data.

4. SUMMARY AND DISCUSSION

In this work, we use data from GRB 160625B to constrain Lorentz violation in the photon sector. The general description of possible photon behaviors, allowing for operators of arbitrary mass dimension d , is predicted in the SME effective field theory for Lorentz violation. The dispersion relation for photons can acquire corrections that depend on polarization, direction of propagation, and energy. Here, we study non-birefringent effects yielding energy- and direction-dependent vacuum dispersion and controlled by coefficients for Lorentz violation with $d = 6, 8, \text{ and } 10$.

Gamma-ray bursts are well suited for these studies because they are distant transient sources involving a range of photon energies and so permit time-of-flight tests. A key challenge in this approach is to distinguish an intrinsic time delay at the source from a time delay induced by Lorentz violation. Most previous studies limit attention to the latter while ignoring possible source-intrinsic effects, which would impact the reliability of the resulting constraints on Lorentz violation. Furthermore, prior limits from gamma-ray bursts are based on the approximate time delay of a single GeV-scale photon. To obtain reliable constraints on Lorentz violation, it is desirable to use the true time delays of broad light curves in different energy multi-photon bands.

GRB 160625B has unusually high photon statistics, allowing the use of amply populated energy bands. Moreover, it is the only burst so far with a well-defined transition from positive to negative spectral lag. This provides a unique opportunity not only to disentangle the intrinsic time delay problem but also to place more reliable constraints on Lorentz violation. Here, we propose that the intrinsic time delay has a positive dependence on the photon energy. Lorentz violation can cause high-energy photons to travel slower than low-energy ones in the vacuum, so the positive correlation of the time delay with energy would gradually become an anticorrelation as the Lorentz violation becomes dominant

TABLE 1
Fit results and estimated 95% C.L. constraints on coefficients for $d = 6, 8, \text{ and } 10$.

	d	6	8	10
Negative spectral lag	τ	$2.44^{+2.37}_{-1.14}$	$3.50^{+3.75}_{-1.69}$	$4.15^{+4.85}_{-2.07}$
	α	$0.11^{+0.05}_{-0.04}$	$0.09^{+0.05}_{-0.04}$	$0.08^{+0.05}_{-0.03}$
	$\sum_{jm} 0Y_{jm}(83.1^\circ, 308^\circ)c_{(l)jm}^{(d)}$	$2.22^{+1.13}_{-1.11} \times 10^{-15} \text{ GeV}^{-2}$	$1.38^{+0.65}_{-0.65} \times 10^{-12} \text{ GeV}^{-4}$	$6.38^{+3.60}_{-3.60} \times 10^{-10} \text{ GeV}^{-6}$
	$\chi^2/\text{d.o.f.}$	76.70/34 = 2.26	74.41/34 = 2.19	77.95/34 = 2.29
Positive spectral lag	τ	$7.09^{+11.47}_{-3.88}$	$6.94^{+10.92}_{-3.72}$	$6.92^{+11.00}_{-3.77}$
	α	$0.05^{+0.04}_{-0.03}$	$0.05^{+0.04}_{-0.03}$	$0.05^{+0.04}_{-0.03}$
	$\sum_{jm} 0Y_{jm}(83.1^\circ, 308^\circ)c_{(l)jm}^{(d)}$	$-6.96^{+6.57}_{-21.17} \times 10^{-17} \text{ GeV}^{-2}$	$-3.71^{+3.50}_{-11.39} \times 10^{-14} \text{ GeV}^{-4}$	$-2.25^{+2.12}_{-6.81} \times 10^{-11} \text{ GeV}^{-6}$
	$\chi^2/\text{d.o.f.}$	93.25/34 = 2.74	93.25/34 = 2.74	93.25/34 = 2.74
95% C.L. bounds	$-2.8 \times 10^{-16} \text{ GeV}^{-2} <$	$\sum_{jm} 0Y_{jm}(83.1^\circ, 308^\circ)c_{(l)jm}^{(6)}$	$< 3.4 \times 10^{-15} \text{ GeV}^{-2}$	
	$-1.0 \times 10^{-15} \text{ GeV}^{-2} <$	$c_{(l)00}^{(6)}$	$< 1.2 \times 10^{-14} \text{ GeV}^{-2}$	
	$-1.5 \times 10^{-13} \text{ GeV}^{-4} <$	$\sum_{jm} 0Y_{jm}(83.1^\circ, 308^\circ)c_{(l)jm}^{(8)}$	$< 2.0 \times 10^{-12} \text{ GeV}^{-4}$	
	$-5.4 \times 10^{-13} \text{ GeV}^{-4} <$	$c_{(l)00}^{(8)}$	$< 7.2 \times 10^{-12} \text{ GeV}^{-4}$	
	$-9.1 \times 10^{-11} \text{ GeV}^{-6} <$	$\sum_{jm} 0Y_{jm}(83.1^\circ, 308^\circ)c_{(l)jm}^{(10)}$	$< 1.0 \times 10^{-9} \text{ GeV}^{-6}$	
	$-3.2 \times 10^{-10} \text{ GeV}^{-6} <$	$c_{(l)00}^{(10)}$	$< 3.5 \times 10^{-9} \text{ GeV}^{-6}$	

at higher energies. By fitting the spectral lag behavior of GRB 160625B, we obtain both a reasonable formulation of the intrinsic energy-dependent time delay and comparatively robust two-sided limits on coefficients for Lorentz violation, as shown in Table 1.

Existing limits on coefficients for Lorentz violation, including photon-sector constraints using other astrophysical sources with the dispersion method, are compiled in Kostelecký & Russell (2017). For the $d = 6$ case, our constraints are somewhat weaker or comparable to existing bounds but can be viewed as comparatively robust. For $d = 8$, only a few limits exist on the 49 coefficients controlling non-birefringent dispersion. Our new bound is linearly independent of these and so helps to constrain the full coefficient space. For $d = 10$, our constraints are the first in the literature. Note that all bounds to date are based on photons with energies far below the Planck scale, and so in principle there is still room for Planck-scale effects.

The 95% C.L. constraints given in Table 1 assume no Lorentz violation in nature and are extracted by considering only one value of d at a time, following the standard practice in the field. However, the presence of multiple values of d could improve the fit. As a proof of principle for this idea, we have performed an analysis allowing the $d = 6, 8, \text{ and } 10$ combinations of coefficients to vary simultaneously. The best-fit values for the three coefficient combinations are found to be approximately $-8.97^{+4.38}_{-4.20} \times 10^{-15} \text{ GeV}^{-2}$, $1.86^{+0.79}_{-0.77} \times 10^{-11} \text{ GeV}^{-4}$, and $-7.00^{+3.23}_{-3.31} \times 10^{-9} \text{ GeV}^{-6}$, respectively, with $\chi^2 = 1.89$ per degree of freedom. It is interesting to note that these nonzero best-fit values are compatible with existing constraints in the literature. Once other gamma-ray bursts displaying spectral-lag transitions become available for similar studies, a definitive search along these lines would become possible. To discover further bursts with spectral-lag transitions, we need to detect larger numbers of GRBs with higher temporal resolutions and more high-energy photons. The up-

coming detectors for gamma-ray observations at very high energies and with higher sensitivity and wider field-of-view, such as the Large High Altitude Air Shower Observatory (Cao 2010, 2014), will be able to detect many high-energy ($> 100 \text{ GeV}$) photons for each luminous GRB. With large statistics for high-energy photons, high-energy light curves with excellent temporal resolutions can be constructed, so the discovery of additional bursts with spectral-lag transitions can be expected. In any case, the future is bright for improving constraints on Lorentz violation using time-of-flight tests from gamma-ray bursts.

This work is supported by the National Basic Research Program (“973” Program) of China (Grant No. 2014CB845800), the National Natural Science Foundation of China (Grant Nos. 11673068, 11603076, and 11103083), the Youth Innovation Promotion Association (2011231 and 2017366), the Key Research Program of Frontier Sciences (QZDB-SSW-SYS005), the Strategic Priority Research Program “Multi-wavelength gravitational wave Universe” (Grant No. XDB23000000) of the Chinese Academy of Sciences, the Natural Science Foundation of Jiangsu Province (Grant No. BK20161096), and the Guangxi Key Laboratory for Relativistic Astrophysics. B.B.Z. acknowledges support from the Spanish Ministry Projects AYA 2012-39727-C03-01 and AYA2015-71718-R. Part of this work used B.B.Z.’s personal IDL code library ZBBIDL and personal Python library ZBBPY. The computation resources used in this work are owned by Scientist Support LLC. L.S. acknowledges support from the Joint NSFC-ISF Research Program (No. 11361140349), jointly funded by the National Natural Science Foundation of China and the Israel Science Foundation. P.M. acknowledges NASA NNX 13AH50G. V.A.K. acknowledges support from the United States Department of Energy under grant DE-SC0010120 and from the Indiana University Center for Spacetime Symmetries.

REFERENCES

- Abdo, A. A., Ackermann, M., Arimoto, M., et al. 2009, *Science*, 323, 1688
 Aharonian, F., Akhperjanian, A. G., Barres de Almeida, U., et al. 2008, *Phys. Rev. Lett.*, 101, 170402

- Amelino-Camelia, G. 2013, *Living Reviews in Relativity*, 16, 5
- Amelino-Camelia, G., Ellis, J., Mavromatos, N. E., Nanopoulos, D. V., & Sarkar, S. 1998, *Nature*, 393, 763
- Band, D. L. 1997, *ApJ*, 486, 928
- Biesiada, M., & Piórkowska, A. 2009, *Classical and Quantum Gravity*, 26, 125007
- Bluhm, R. 2006, *Lecture Notes in Physics*, 702, 191
- Boggs, S. E., Wunderer, C. B., Hurley, K., & Coburn, W. 2004, *ApJ*, 611, L77
- Burns, E. 2016, *GRB Coordinates Network*, 19581
- Cheng, L. X., Ma, Y. Q., Cheng, K. S., Lu, T., & Zhou, Y. Y. 1995, *A&A*, 300, 746
- Cao, Z. 2010, *Chinese Physics C*, 34, 249
- Cao, Z. 2014, *Nuclear Instruments and Methods in Physics Research A*, 742, 95
- Colladay, D., & Kostelecký, V. A. 1997, *Phys. Rev. D*, 55, 6760
- . 1998, *Phys. Rev. D*, 58, 116002
- Dirrsa, F., Racusin, J., McEnery, J., & Desiante, R. 2016, *GRB Coordinates Network*, 19580
- Ellis, J., & Mavromatos, N. E. 2013, *Astroparticle Physics*, 43, 50
- Ellis, J., Mavromatos, N. E., Nanopoulos, D. V., Sakharov, A. S., & Sarkisyan, E. K. G. 2006, *Astroparticle Physics*, 25, 402
- Fermi LAT, V. V. f. t., & GBM Collaborations. 2010, *ArXiv e-prints*, arXiv:1008.2913
- Foreman-Mackey, D., Hogg, D. W., Lang, D., & Goodman, J. 2013, *PASP*, 125, 306
- Gubitosi, G., Pagano, L., Amelino-Camelia, G., Melchiorri, A., & Cooray, A. 2009, *JCAP*, 8, 021
- Jacob, U., & Piran, T. 2008, *JCAP*, 1, 031
- Kislat, F., & Krawczynski, H. 2015, *Phys. Rev. D*, 92, 045016
- Kislat, F., & Krawczynski, H. 2017, *Phys. Rev. D*, 95, 083013
- Kostelecký, V. A. 2004, *Phys. Rev. D*, 69, 105009
- Kostelecký, V. A., & Mewes, M. 2001, *Phys. Rev. Lett.*, 87, 251304
- . 2002, *Phys. Rev. D*, 66, 056005
- . 2006, *Phys. Rev. Lett.*, 97, 140401
- . 2007, *Phys. Rev. Lett.*, 99, 011601
- . 2008, *ApJ*, 689, L1
- . 2009, *Phys. Rev. D*, 80, 015020
- . 2013, *Phys. Rev. Lett.*, 110, 201601
- Kostelecký, V. A., & Potting, R. 1991, *Nuclear Physics B*, 359, 545
- . 1995, *Phys. Rev. D*, 51, 3923
- Kostelecký, V. A., & Russell, N. 2017, *ArXiv e-prints*, arXiv:0801.0287v10
- Kostelecký, V. A., & Samuel, S. 1989, *Phys. Rev. D*, 39, 683
- Laurent, P., Götz, D., Binétruy, P., Covino, S., & Fernandez-Soto, A. 2011, *Phys. Rev. D*, 83, 121301
- MAGIC Collaboration, Albert, J., Aliu, E., et al. 2008, *Physics Letters B*, 668, 253
- Mattingly, D. 2005, *Living Reviews in Relativity*, 8, 5
- Minaev, P. Y., Pozanenko, A. S., Molkov, S. V., & Grebenev, S. A. 2014, *Astronomy Letters*, 40, 235
- Norris, J. P., Nemiroff, R. J., Bonnell, J. T., et al. 1996, *ApJ*, 459, 393
- Pavlopoulos, T. G. 2005, *Physics Letters B*, 625, 13
- Planck Collaboration, Ade, P. A. R., Aghanim, N., et al. 2014, *A&A*, 571, A16
- Shao, L., Zhang, B.-B., Wang, F.-R., et al. 2016, *ArXiv e-prints*, arXiv:1610.07191
- Stecker, F. W. 2011, *Astroparticle Physics*, 35, 95
- Tasson, J. D. 2014, *Reports on Progress in Physics*, 77, 062901
- Toma, K., Mukohyama, S., Yonetoku, D., et al. 2012, *Phys. Rev. Lett.*, 109, 241104
- Vasileiou, V., Jacholkowska, A., Piron, F., et al. 2013, *Phys. Rev. D*, 87, 122001
- Wei, J.-J., Zhang, B.-B., Shao, L., Wu, X.-F., & Mészáros, P. 2017, *ApJ*, 834, L13
- Xu, D., Malesani, D., Fynbo, J. P. U., et al. 2016, *GRB Coordinates Network*, 19600
- Zhang, B.-B., Zhang, B., Castro-Tirado, A. J., et al. 2016, *ArXiv e-prints*, arXiv:1612.03089